INTERNATIONAL JOURNAL OF APPLIED RESEARCH ON TEXTILE
URL: http://atctex.org/ijartex
Volume 4, Issue 1, pp 23-32, September 2016

DIELECTRIC BEHAVIOUR MODELLING OF THE FABRIC COATED WITH NANOCOMPOSITES

ABID K*, DHOUIB S, SAKLI F.

LABORATOIRE DE GENIE TEXTILE, UNIVERSITE DE MONASTIR, TUNISIA

Received 23 September 2015, Accepted 27 February 2016

ABSTRACT

In this paper, the dielectric properties of coated fabric by nanocomposites have been studied. In fact, a resin/clay mixture was deposited on a 100 % cotton fabric and tested using a dielectric impedance spectrometer device for measuring the dielectric permittivity. The enhancement of fabric dielectric properties was noticed by calculating the complex permittivity. It has been concluded that the increasing quantities of clay and resin, decrease significantly the dielectric permittivity of a 400 g/m^2 sergé fabric 100% cotton. Moreover it has been noted that the Havriliak and Négami model could be applied for these hybrid fabrics for a precise frequency spectrum.
The mathematical equation has proved to be effective in predicting the fabric dielectric permittivity, by calculation the constants referred to this model. The result of theses computations indicates that clay application in nanocomposites proved its importance because the dielectric properties of the fabric are really enhanced according to the clay percentage in the coating by maximising the loss of ε''.

KEY WORDS

Nanocomposite, Resin, Modelling, Polyacrylate and Dielectric.

1. INTRODUCTION

A dielectric materials measurement can provide critical design parameter information for many electronics applications. For example, the loss of a cable insulator, the impedance of a substrate, or the frequency of a dielectric resonator can be related to its dielectric properties. Over the past 50 years, there have been numerous attempts to measure the complex permittivity of dielectric materials at large spectrum of frequencies employing waveguides, resonators, and broadband dispersive Fourier transform spectroscopic technique (Linhart et al.,1956; Champlin et al., 1961; Champlin et al., 1967; Champlin et al., 1966; Dmowski et al., 1980; Afsar et al., 1994; Parshin et al., 1995). More recent applications in the area of aerospace, automotive, food and medical industries have also been found to benefit from knowledge of dielectric properties (Champlin et al., 1967; Champlin et al., 1966; Dmowski et al., 1980).

Dielectric permittivity is a complex function having real and imaginary components. The real part of dielectric permittivity is usually expressed as dielectric constant (ε'), which is the ratio of the electric-field storage capacity of a material to that of free space. The imaginary part of dielectric permittivity is usually expressed as dielectric loss, which represents attenuation and dispersion (Dobson et al., 1985;

* : Corresponding author. Email : kaledabid2003@yahoo.fr

Dolphin et al., 1978; Keller et al., 1989; Knight et al., 1990; Knoll et al., 1996). In fact there are many models that have been studied by many researchers like Debye, Cole -Cole, Havriliak-Negami, and Lorenz (Debye, 1912; Cole et al., 1941; Havriliak et al., 1967; Oughstun et al., 2003).

In previous work, various tests of application performance on fabrics coated with nanocomposites such as mechanical properties, heat insulation and many other properties have been studied (Abid et al., 2011; Abid et al., 2010; Dhouib et al., 2012).

The purpose of this study is:

- First, to make nanocomposites: this is considered very delicate because the commercial used resins are frequently mixed with water (problem of mixing with clay which is very hydrophilic). In addition, the analysis of DRX patterns requires a lot of care because the multitude of the spectrum of the different clays is superposed and difficult to analyse.

- Second, to show how the nanocomposite coatings on fabrics are carried out and enhance the dielectric properties of this new hybrid fabric in conjunction with the clay percentage and the deposited quantity.

- Third and finally to modulate the found results in the appropriate model.

2. METHODOLOGY

Tunisian natural clay was directly extracted from the soil, crushed, and dried for 48 h in an oven (60°C). Impurities, like little stones, were eliminated from the clay. Then, the clay was filtered through a riddle (with a hole diameter < 0.1 mm) three times until a very fine product was obtained.
In order to have a good dispersion of the clay particles, we must have 10 g of Tunisian clay in which 100 mL of methylene chloride (CH_2CL_2) is added, and ultrasonicated for 2 h at 25°C (freq.=28 KHz). Then, the prepared clay solution was very gradually added to the resin with different percentages of clay (3% to 10 %), and 24 h.
Different mixtures of resin/clay were deposited on (400 g/m²) cotton fabric (sergé of 3) by using a 40 mesh printing flat frame. The polymerisation of these coatings was carried out at 150°C for 5 min (Abid et al., 2010), and afterwards, 5 min of drying was carried 100 - out in order to evaporate the water and CH_2CL_2. The coatings were observed by SEM to confirm the formation of nanocomposites. Then, the dielectric permittivities of the coated materials (three trials for each sample; σ = 0.05 %) were determined by using a dielectric impedance spectrometer device.

3. RESULTS

Table 1 gives the characteristics of the prepared samples:

Table 1: Description of the prepared samples.

Sample N°	Description	Thickness (mm)	Deposited quantity
	Reference	0.533	0
0	Clay 0%	0.552	26.0
1	Clay 3%	0.623	130.8
2	Clay 3%	0.657	140.8
3	Clay 5%	0.587	88.5
4	Clay 5%	0.590	96.2
5	Clay 8%	0.610	96.2
6	Clay 8%	0.677	148.5
7	Clay 10%	0.647	193.1

In addition to the x-ray diffraction (XRD) results which had been presented in our previous work (Abid et al., 2010) and to validate the morphology of the nanocomposites, the internal nanometer-scale structure was observed by SEM, which provides direct visualisation of the morphology, spatial phase distribution, and structural effects of a selected sample area.

Figure 1 represents the SEM images of the obtained nanocomposite resin/clay, which shows that the clay is well intercalated in the organic matrix, and forms unique structure of the new hybrid material. The dark zones represent the organic matrix and the bright zones represent the mineral charge (clay) which is well mixed in the organic matrix (Anastasiadis et al., 2000).

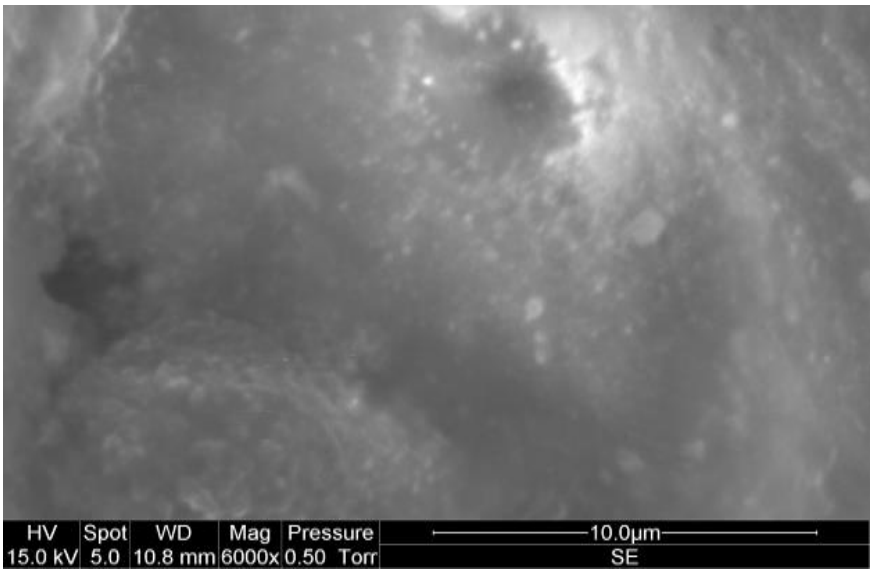

Figure 1: SEM image of nanocomposite PAC/clay.

Besides that, the chemical composition inside any dark zone (organic phase) on the SEM images showed the presence of clay elements (magnesium (Mg), potassium (K), aluminium (Al), and silicon (Si)) (Figure 3). Since the composition of the organic resins can only contain carbon (C), hydrogen (H), and oxygen (O), the clay presence in these zones is confirmed to be inside the structure of the organic matrix which again the formation of nanocomposites. The same task for the bright zone (Figure 2, mineral phase) is shown to confirm the presence of resin components (C, H, and O).

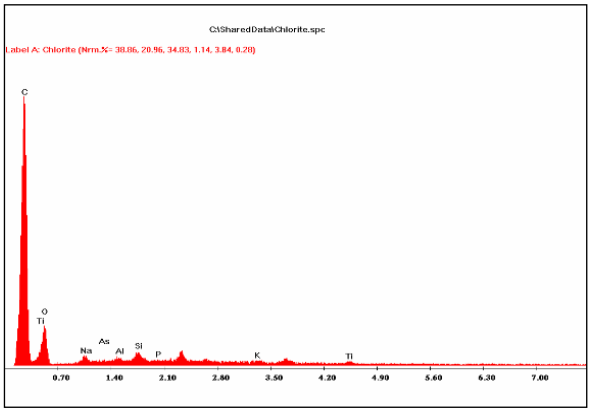

Figure 2: Composition analysis of nanocomposite PAC/clay in the bright zone.

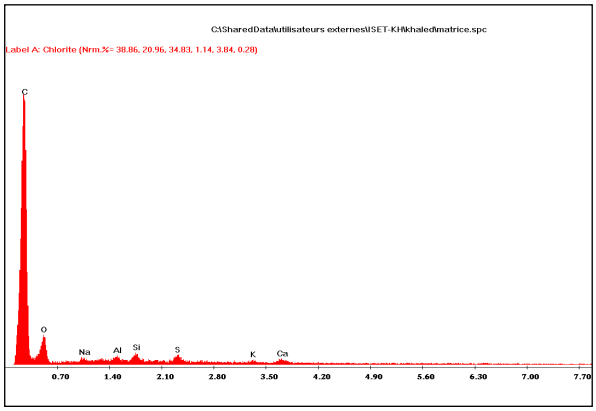

Figure 3: Composition analysis of nanocomposite PAC/clay in the dark zone.

4. THEORETICAL BACKGROUND

In this paragraph we attempted to do some measurements of some parameters having a close link with materials' dielectric properties and more precisely the complex permittivities as the electrical conductivities and resistances have already been studied in a previous work. We used a dielectric impedance spectrometer device and we reached the complex permittivities introduced in table 2.

We chose the Havriliak and Négami model which is quite general and which can be applied to all polymeric materials (figure 4).

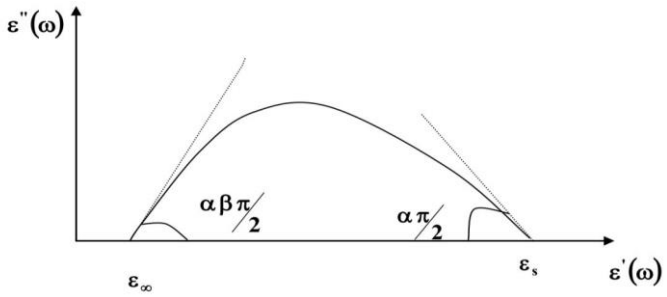

Figure 4: Representation of Havriliak and Négami's equation (Havriliak et al., 1966).

The equation expressing this behaviour is the following:

$$\varepsilon(\omega) = \varepsilon_\infty + \frac{\Delta\varepsilon}{(1+(i\omega\tau)^\alpha)^\beta}$$

Where:

ε(ω) : complex permittivity,

ε_∞: real permittivity as pulsation tends towards ∞,

ε_s: real permittivity as pulsation tends towards 0,

$\Delta\varepsilon = \varepsilon_s - \varepsilon_\infty$

ω: pulsation,

ζ: time constant,

α, β: constants used in the model.

5. RESULTS AND DISSCUSSIONS

To start with, we wanted to have an idea about the variations of the curves translating the imaginary permittivity in conjunction with the frequency. This will show us if there is any influence of nanocomposites on materials' dielectric behaviour. This will also allow us to see if it's possible to reduce the loss of resistivity at a low frequency. This can be achieved by verifying ε'' (figure 5).

Table 2: Real and imaginary permittivities in conjunction with log(frequency).

		Sample		Sample		Sample		Sample		Sample		Sample		Sampl		Sample 0		Reference	
Log(Fr	Freq	ε’	ε’’	ε’	ε’’	ε’	ε’’	ε’	ε’’	ε’	ε’’	ε’	ε’’	ε’	ε’	ε’	ε’’	ε’	ε’’
6.0	10000	3.4	0.4	3.5	0.5	3.0	0.3	2.8	0.3	2.9	0.3	3.0	0.3	2.9	0.	2.7	0.3	2.5	0.2
5.8	66667	3.5	0.5	3.6	0.5	3.0	0.3	2.9	0.4	3.0	0.3	3.1	0.4	3.0	0.	2.8	0.3	2.5	0.3
5.6	44444	3.7	0.6	3.7	0.6	3.1	0.4	3.0	0.4	3.0	0.4	3.2	0.4	3.1	0.	2.9	0.4	2.6	0.3
5.5	29630	3.8	0.6	3.9	0.6	3.2	0.4	3.1	0.5	3.1	0.4	3.3	0.5	3.2	0.	3.0	0.4	2.7	0.3
5.3	19753	4.0	0.7	4.0	0.7	3.3	0.5	3.2	0.6	3.2	0.5	3.4	0.5	3.4	0.	3.1	0.5	2.7	0.4
5.1	13169	4.2	0.8	4.2	0.8	3.4	0.6	3.4	0.7	3.4	0.6	3.6	0.6	3.5	0.	3.2	0.5	2.8	0.4
4.9	87792	4.4	0.9	4.4	0.9	3.6	0.6	3.5	0.8	3.5	0.6	3.7	0.7	3.7	0.	3.3	0.6	2.9	0.5
4.8	58528	4.6	1.1	4.6	1.1	3.7	0.7	3.7	0.9	3.7	0.7	3.9	0.8	3.9	0.	3.5	0.7	3.1	0.6
4.6	39018	4.9	1.2	4.9	1.2	3.9	0.8	3.9	1.0	3.8	0.8	4.1	0.9	4.1	1.	3.6	0.8	3.2	0.7
4.4	26012	5.2	1.4	5.2	1.4	4.1	1.0	4.2	1.2	4.0	1.0	4.3	1.0	4.3	1.	3.8	1.0	3.4	0.8
4.2	17342	5.5	1.6	5.6	1.6	4.3	1.1	4.5	1.4	4.3	1.1	4.6	1.2	4.6	1.	4.0	1.2	3.5	0.9
4.1	11561	5.9	1.8	6.0	1.8	4.6	1.3	4.8	1.6	4.5	1.3	4.9	1.3	4.9	1.	4.3	1.4	3.7	1.1
3.9	7707	6.4	2.0	6.4	2.0	4.9	1.5	5.2	1.9	4.9	1.5	5.2	1.5	5.3	1.	4.6	1.7	4.0	1.2
3.7	5138	6.9	2.2	7.0	2.2	5.3	1.7	5.7	2.2	5.2	1.7	5.6	1.8	5.7	1.	5.0	2.0	4.3	1.5
3.5	3425	7.6	2.5	7.6	2.5	5.8	2.0	6.3	2.5	5.7	2.0	6.1	2.0	6.2	2.	5.4	2.4	4.6	1.8
3.4	2283	8.3	2.7	8.3	2.7	6.3	2.3	7.0	2.9	6.2	2.2	6.6	2.2	6.8	2.	5.9	2.9	5.0	2.1
3.2	1522	9.0	2.9	9.1	2.9	6.9	2.6	7.8	3.2	6.8	2.5	7.3	2.5	7.4	2.	6.6	3.6	5.4	2.6
3.0	1015	9.9	3.0	9.9	3.0	7.7	3.0	8.8	3.4	7.6	2.8	8.0	2.6	8.1	2.	7.3	4.4	6.0	3.2
2.8	676	10.	3.1	10.	3.1	8.5	3.2	9.8	3.6	8.4	3.0	8.7	2.7	8.8	2.	8.3	5.5	6.6	3.9
2.7	451	11.	3.1	11.	3.1	9.4	3.5	10.	3.7	9.2	3.1	9.5	2.8	9.5	2.	9.4	6.8	7.3	4.9
2.5	300	12.	3.1	12.	3.0	10.	3.6	11.	3.7	10.	3.2	10.	2.8	10.	2.	10.	8.5	8.2	6.1
2.3	200	13.	3.1	13.	3.0	11.	3.6	12.	3.6	11.	3.2	11.	2.8	10.	2.	12.	10.5	9.3	7.8
2.1	133	14.	3.0	14.	2.9	12.	3.6	13.	3.5	11.	3.2	11.	2.7	11.	2.	15.	13.1	10.	10.1
1.9	89.	14.	2.9	14.	2.8	13.	3.6	14.	3.4	12.	3.1	12.	2.6	11.	2.	18.	16.1	12.	13.1
1.8	59	15.	2.9	15.	2.8	14.	3.6	15.	3.3	13.	3.0	13.	2.5	12.	2.	21.	19.8	14.	17.2
1.6	39	16.	2.8	16.	2.7	15.	3.6	16.	3.2	14.	3.0	13.	2.4	12.	1.	26.	24.1	17.	22.7
1.4	26	17.	2.7	16.	2.7	16.	3.5	17.	3.2	15.	2.9	14.	2.3	13.	1.	31.	29.1	20.	30.1
1.2	17	17.	2.7	17.	2.7	17.	3.6	17.	3.2	15.	2.9	15.	2.2	13.	1.	38.	35.3	24.	40.4
1.1	11	18.	2.6	18.	2.8	17.	3.6	18.	3.3	16.	2.8	15.	2.1	14.	1.	45.	43.1	30.	54.3
0.9	7.	19.	2.5	18.	2.9	18.	3.7	19.	3.6	17.	2.8	16.	2.1	14.	1.	53.	53.3	37.	73.6
0.7	5	19.	2.5	19.	3.0	19.	3.9	19.	4.1	17.	2.9	16.	2.1	14.	1.	62.	67.4	47.	100.
0.5	3	20.	2.6	20.	3.3	20.	4.3	20.	4.8	18.	2.9	17.	2.1	15.	1.	72.	87.2	59.	138.
0.4	2	20.	2.7	20.	3.7	21.	4.8	21.	5.8	19.	3.1	17.	2.1	15.	2.	84.	114.	74.	191.
0.2	1	21.	2.9	21.	4.3	22.	5.5	22.	7.4	19.	3.4	18.	2.2	16.	2.	99.	154.	95.	266.
0.0	1	21.	3.4	22.	5.1	23.	6.6	23.	9.6	20.	3.8	18.	2.3	16.	2.	117	208.	121	372.
-0.2	0	22.	4.0	23.	6.1	24.	8.1	24.	12.	21.	4.4	19.	2.5	17.	2.	141	287.	155	524.
-0.3	0	22.	4.9	24.	7.4	26.	9.9	27.	16.	21.	5.2	19.	2.7	17.	3.	172	395.	202	744.
-0.5	0	23.	6.2	26.	9.0	28.	12.	30.	20.	22.	6.3	20.	3.1	18.	4.	214	546.	263	1060
-0.7	0	24.	7.9	28.	11.	31.	14.	34.	25.	23.	7.8	20.	3.2	18.	5.	266	749.	342	1508
-0.9	0	25.	10.	30.	13.	34.	17.	38.	31.	25.	9.8	21.	3.6	19.	6.	336	1035	448	2143
-1.0	0	25.	11.	31.	14.	37.	18.	41.	34.	25.	11.	21.	4.0	20.	7.	401	1307	549	2776

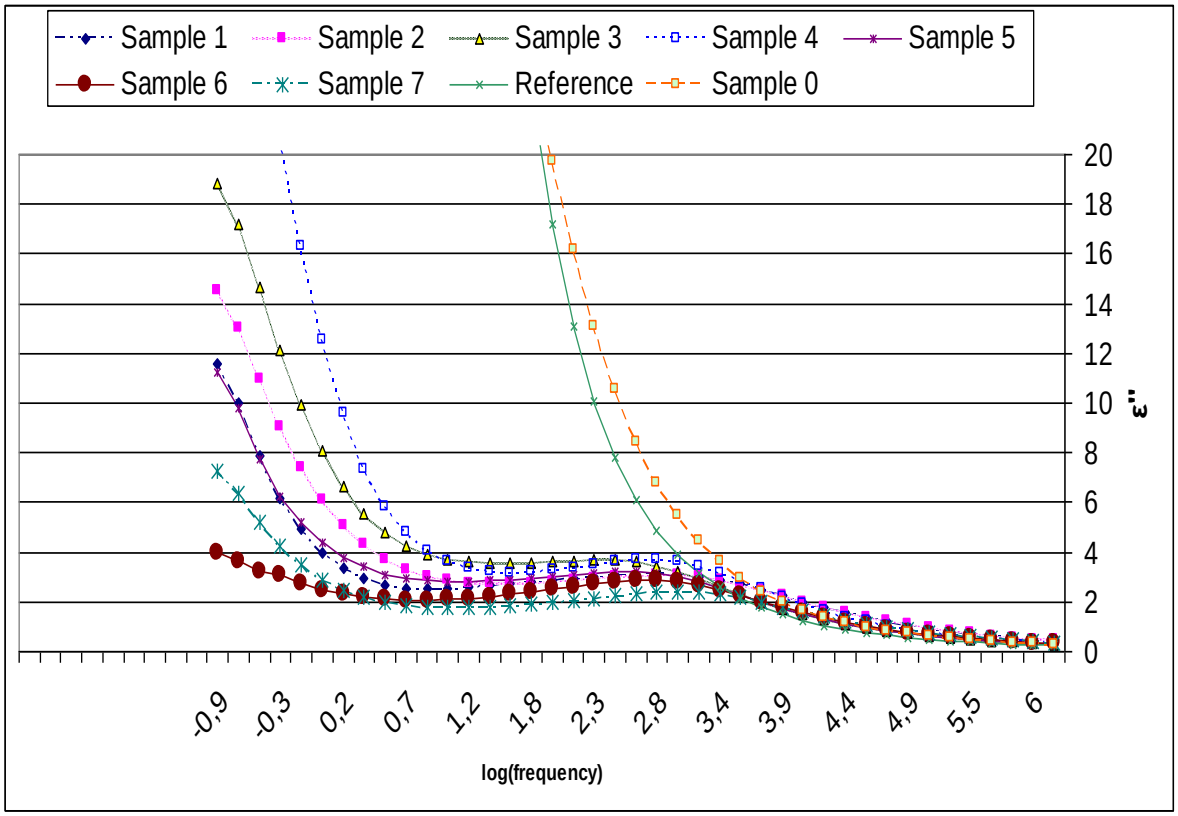

Figure 5: Imaginary permittivity in conjunction with log(frequency).

We can conclude that for the reference and sample 0, the two curves are almost combined when the frequency is below 100 Hz. Between 100 Hz and 10 KHz, sample 0 shows higher losses, than those of the reference. Above 10 KHz the two curves tend to get closer to each other. This is true up to 1 MHz. This is probably due to the penetration of the resin into the fabric which causes the replacement of air by the resin in the intra-yarn and inter-yarn pores. For frequencies ranging from 0,1 to 10 KHz, the resin seems to have an important impact on the hybrid material's conductivity. However, this loss does not exceed 20%. The remaining samples display even lower permittivities at low frequencies. This loss gets higher as we move from sample 4 to 1. For a fixed frequency, the lower the nanocomposite quantity the lower the permittivity. As for samples 7 and 6, we can notice that their permittivities are very low compared to the other samples. We can therefore conclude that starting from a certain rate of nanocomposites there is a remarquable improvement in the material's resistivity. Sample 6 is a case in point.

6. MODELLING

In the following paragraph, we drew the curves representing the imaginary permittivities in conjunction with the real ones (figure 6).

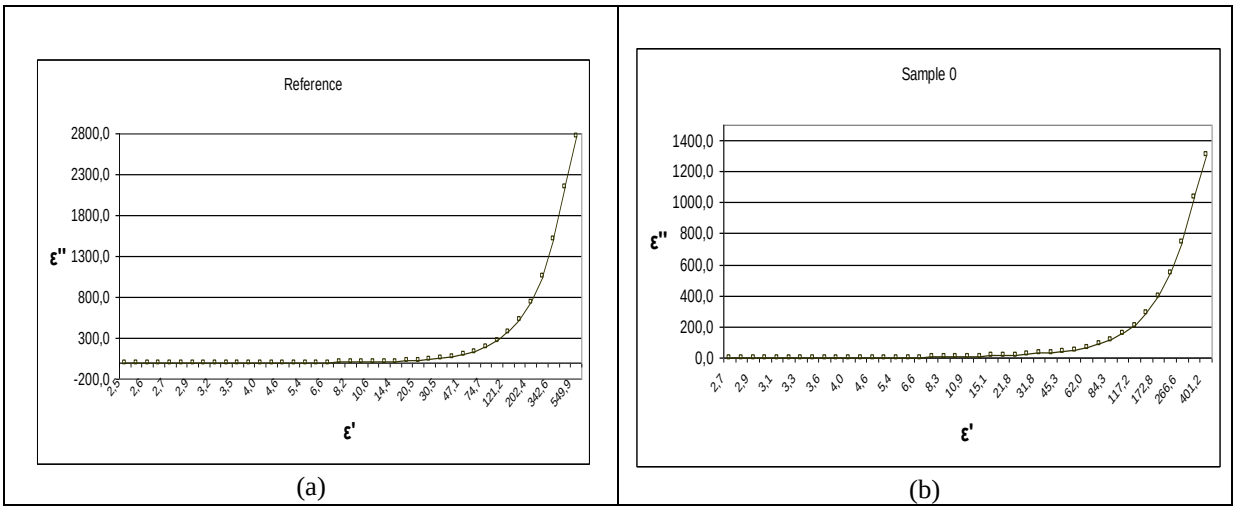

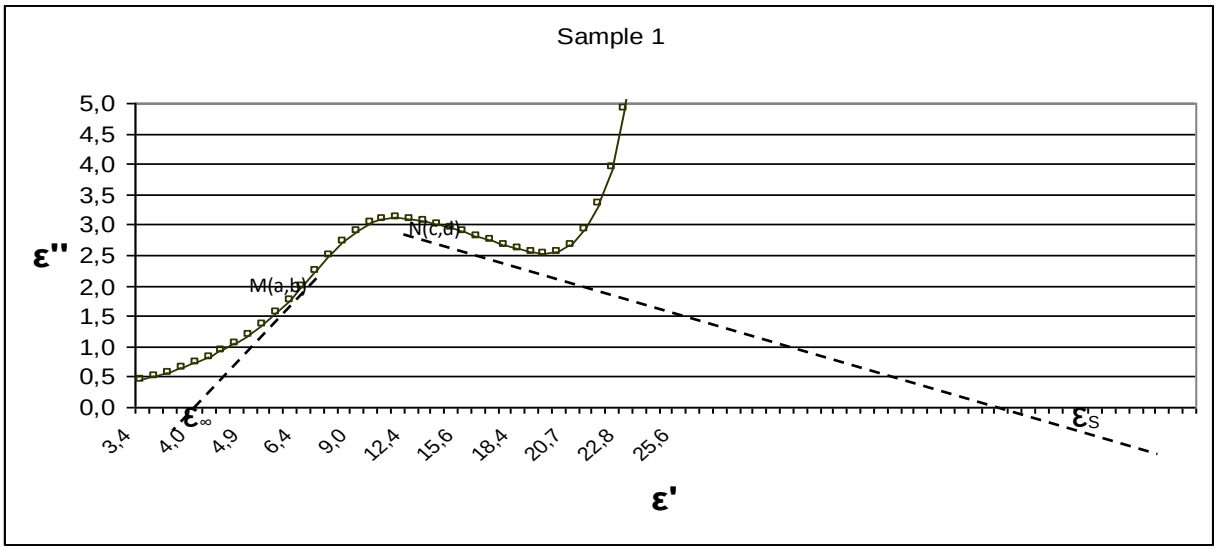

(c)

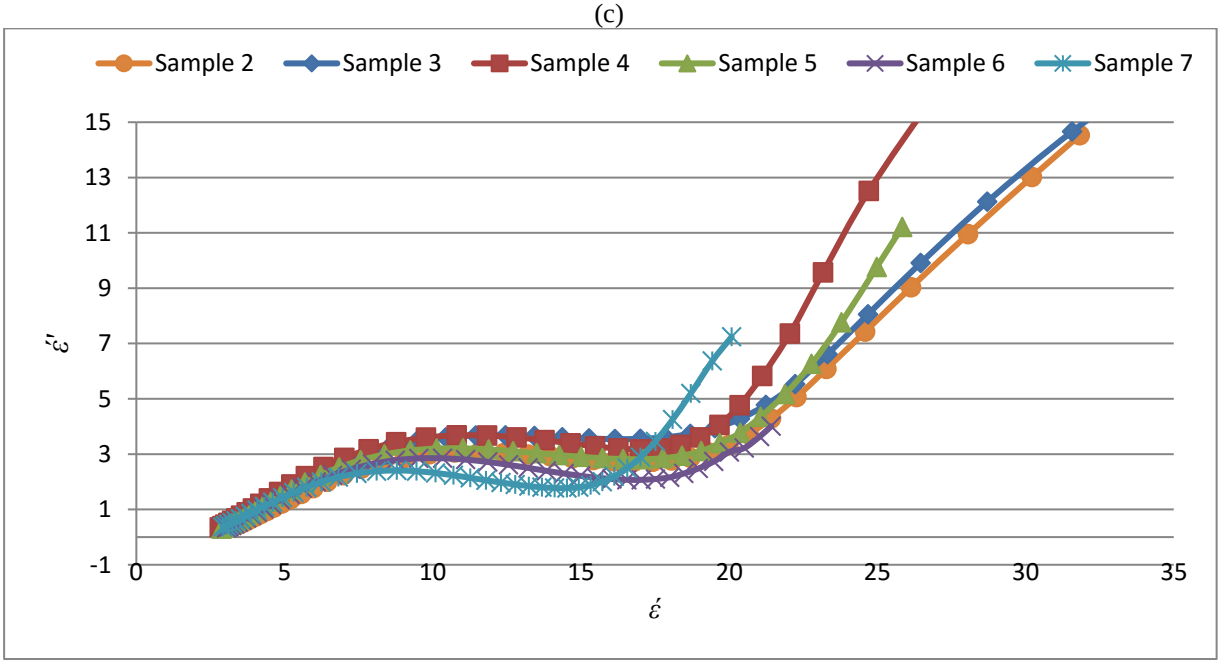

(d)

Figure 6 (a-d): Representation of the imaginary permittivity in conjunction with the real permittivity.

We can notice that for the sample 0 and the reference, there is no model that can describe this behaviour in any event for the frequencies between 0.1 Hz and 1MHz. For the rest of the samples in which we put the clay in order to make nanocomposites, the general variations of the corresponding curves began to have a certain shape that recall the Havriliak and Négami model within a certain frequency spectrum (between 200 KHz and 40 Hz). This spectrum is incidentally equivalent for all samples. In order to calculate the parameters displayed in table 3, an illustration of an example on figure 6-c is presented.
Using ORIGIN, $tg\alpha\pi/2$ and $tg\alpha\beta\pi/2$ were determined by measuring the opposite side and the adjacent side on the samples' curves, and then α, β were deduced.
ε_∞ and ε_s were determined by using the tangent equations as follows:

$$\varepsilon_\infty = a - b/tg(\alpha\pi/2)$$

$$\varepsilon_s = c - d/tg(\pi - arctg(\alpha\beta\pi/2))$$

Knowing these parameters, the Havriliak and Négami equations of all samples were determined (table3).

Table 3: Determination of Havriliak and Négami equations' parameters.

Sample	a	b	α	β	ε_∞	c	d	ε_s	$\tau(ms) = 1/\omega_0$	Complex permittivity ε(ω)
Reference	X	X	X	X	X	X	X	X	X	X
0	X	X	X	X	X	X	X	X	X	X
1	5.90	1.80	0.24	0.26	1.35	16.30	2.8	44.4	128	$1.35+43/(1+(i128\omega)^{0.24})^{0.26}$
2	6.00	1.80	0.24	0.69	1.45	14.70	2.8	25.4	192	$1.45+24/(1+(i129\omega)^{0.24})^{0.69}$
3	5.80	2.00	0.29	0.1	1.72	14.40	3.6	90.8	333	$1.72+89/(1+(i333\omega)^{0.29})^{0.1}$
4	5.70	2.20	0.28	0.28	1.02	15.50	3.3	42.0	128	$1.02+41/(1+(i128\omega)^{0.28})^{0.28}$
5	5.70	2.00	0.22	0.26	0.14	14.30	3.0	47.1	3.3	$0.14+47/(1+(i3.3\omega)^{0.22})^{0.26}$
6	5.60	1.80	0.21	0.47	0.34	14.40	2.3	29.1	3.3	$0.34+29/(1+(i3.3\omega)^{0.21})^{0.47}$
7	5.70	1.80	0.31	0.33	2.30	10.70	2.2	24.3	1	$2.3+22/(1+(i\omega)^{0.31})^{0.33}$

It becomes clear that when we coat a fabric with nanocomposites, its dielectric behaviour begin to reach certain conformity to the Havriliak and Negami model. This is true for a precise spectrum of frequency.
Clay addition to the resin enables, for low frequencies, the real permittivity to decrease 20 times, and, the imaginary one 200 times (means resistivity gain). This is very useful in the case of manufacturing protective clothes of high voltage manipulators.

7. CONCLUSIONS

In this work, it has been concluded that for the reference and the sample which has been coated only with polyacrylate resin, and between 0.1 Hz and 1 MHz, there is no model that can explain their behaviour. In fact, we obtain two curves characterised by an exponentially tendency in conjunction with the frequency. That means the lower the frequency the lower the electric resistivity. Besides, and for the rest of the samples which have been coated with nanocomposites, the variation of the corresponding curves shows a peak corresponding to the time constant ζ.

It has been shown, by computing, that a nanocomposite coating can be attributed to a Havriliak and Négami model for the frequencies ranging from 200 KHz to 40 Hz (limit of the model validity), and beyond this values, there is surely another model that can be applied. Using this model equations, all its parameters have been determined (α, β, ζ, ε_s, and ε_∞).

Knowing these general equations, real and imaginary permittivities could be deduced and the behaviour of these hybrid materials could be predicted.

The real permittivities at the frequencies limits (ε_s and ε_∞) can't unfortunately inform us about the dielectric behaviour at high or low frequencies (direct current $\omega = 0$) because the model can't be applied at these limits.

Supplementary studies in a large spectrum of frequencies seem to be crucial to understand and to define more the behaviour of such materials.

REFERENCES

Abid K, Dhouib S & Sakli F. (2010), Modelling of Thermal Behaviour of a Fabric Coated With Nanocomposites. *Journal of Applied Science*, (10) 1, 71–74.

Abid, K., Dhouib, S., Sakli, F. (2010), Addition Effect of Nanoparticles on the Mechanical Properties of Coated Fabric. *The Journal of the textile institute*. (101) 5, 443 - 451.

Abid, K., Dhouib, S., Sakli, F. (2011), Mechanical Modelling of Materials Coated With Nanocomposites. *The Journal of the textile institute*. (102) 2, 157 - 163.

Afsar, M N., Chi, H. (1994), Millimeter wave complex refractive index, complex dielectric permittivity and loss tangent of extra high purity and compensated silicon. *International Journal of Infrared Millimeter Waves*. (15) 7, 1181–1188.

Anastasiadis, S H., Karatasos, K., Vlachos, G., Manis, E., Giannelis, E P. (2000), Nanoscopic-Confinement Effects on Local Dynamics. *Physical Review Letters*. (84), 290 - 915.

Champlin, K S., Krongard, R R. (1961), the measurement of conductivity and permittivity of semiconductor spheres by an extension of the cavity perturbation method. *IRE Transactions on Microwave Theory and Techniques*. (MTT-9). (11), 545–551.

Champlin, K S., Holm, J D., Glover, G H. (1967), Electrodeless determination of semiconductor conductivity from TE01 —Mode reflectivity. *Journal of Applied Physics*. (38) 1, 96–98.

Champlin, K S., Glover G H. (1966), Influence of waveguide contact on measured complex permittivity of semiconductors. *Journal of Applied Physics*. (37) 6, 2355–2360.

Cole, K S., Cole, RH. (1941), Dispersion and Absorption in Dielectrics - I Alternating Current Characteristics. *Journal of Chemistry and Physics*. (9) 1, 341–352

Debye, P. (1912), Zur Theorie der spezifischen Waerme. *Zur Annalen der Physik* (in German) (Leipzig). (39) 4, 789.

Dmowski, S., Krupka, J., Milewski, A. (1980), Contactless IEEE Trans Instrum Meas. *IEEE Transaction on Instrumentation Measurement*. (IM-29). (1), 67–70.

Dhouib, S., Abid, K., Sakli, F. (2010), Study of Thermal Behaviour of Fabric Coated With Nanocomposites Polyacrylate/Clay. *Journal of applied science*. (16) 3, 101 - 110.

Dobson, M. C., Ulaby, F. T., Hallikainen, M. T., & El-Rayes, M. A. (1985). Microwave dielectric behavior of wet soil—Part II: Dielectric mixing models.*IEEE Trans. Geosci. Remote Sens*, *23*(1), 35-46.

Dolphin, L T., Beatty, W B., Tanzi, J D. **(1978)**, Radar probing of Victorio Peak. *New Mexico Geophysics.* (43) 7, 1441–1448.

Havriliak, S., Négami, S. **(1966)**, A complex plane analysis of α-dispersions in some polymer systems. *Journal of Polymer Science*. (14) 1, 99.

Havriliak, S., Negami, S. (1967), A complex plane representation of dielectric and mechanical relaxation processes in some polymers. *Polymers*. (8) 1, 161–210.

Keller, G V. (**1989**), Electrical properties; in, Practical Handbook of Physical Properties of Rocks and Minerals, ed (Boca Raton, FL, CRC Press),.

Knight, R., Endres, A. (**1990)**, A new concept in modeling the dielectric response of sandstones: defining a wetted rock and bulk water system. *Geophysic*. (55) 5, 586– 594.

Knoll, M D. (1996), A petrophysical basis for ground-penetrating radar and very early time electromagnetics, electrical properties of sand-clay mixtures. *Unpub PhD disser.* University of British Columbia, 316.

Linhart, J G., Templeton, I M., Dunsmuir, R. (1956), A microwave resonant Cavity method for measuring the resistivity of semiconducting Materials. *British Journal of Applied Physics*. (7) 1, 36–37.

Oughstun, K E., Cartwright, N A. (2003), On the Lorentz-Lorenz formula and the Lorentz model of dielectric dispersion. *Optics Express*. (11) 1, 1541-1546.

Parshin, V V., Heidinger, R., Andreev, B A., Gusev, A V., Shmagin, V B. (1995), Silicon as an advanced window material for high power gyrotrons. *International Journal of Infrared Millimeter Waves*. (16) 5, 863-869.